International Journal of GEOMATE, March., 2024 Vol.26, Issue 115, pp.81-88
ISSN: 2186-2982 (P), 2186-2990 (O), Japan, DOI: https://doi.org/10.21660/2024.115.g13208
Geotechnique, Construction Materials and Environment

INVESTIGATION OF STRESS BEHAVIOR IN EMBANKMENT DUE TO RAINFALL INFILTRATION

Daiki Yamashita[1], *Shin-ichi Kanazawa[2], Hayato Suzuki[1] and Kira Iida[1]

[1]Graduate School of Science and Technology Niigata University, Japan;
[2]Faculty of Engineering, Niigata University, Japan

*Corresponding Author, Received: 07 July 2023, Revised: 21 Feb. 2024, Accepted: 22 Feb. 2024

ABSTRACT: In recent years, sudden heavy rains due to climate change have increased, and there are many cases of collapse of soil structures. In particular, embankment structures are social infrastructure structures that are essential to our lives, so the damage caused by their collapse is enormous, and it is necessary to prevent this from happening. However, the factors and mechanisms leading to the collapse of embankment structures have not been sufficiently analyzed and elucidated, and elucidation is urgently needed. Therefore, in this study, we conducted an embankment model experiment focusing on rainfall and a reproduction analysis using the air-dissolved unsaturated soil/water/air-coupled finite analysis code in an attempt to understand the moisture state and stress behavior of the embankment due to rainfall. As a result, through model experiments, we were able to confirm that rainfall penetrates from the embankment crest and the slope, causing the embankment to collapse from near the toe of the slope, and it was clarified that this is the mechanism by which the embankment collapses due to rainfall. In addition, the reproduction analysis confirmed qualitative agreement with the model experiment and clarified the usefulness of this analysis code. Furthermore, the stress behavior of the embankment, which is difficult to clarify through experiments, was clarified. In this way, the internal conditions and collapse mechanisms of embankments due to rainfall were elucidated using two methods: experiment and analysis.

Keywords: Embankment, Rainfall infiltration, Model experiment, Numerical Analysis

1. INTRODUCTION

In recent years, torrential rain due to climate change and sudden heavy rain, such as typhoons, are increasing. According to the Japan Meteorological Agency [1], over the 50 years until 2022, heavy rainfall of 50 mm/hour or more has increased 1.65 times, and heavy rain of 80 mm/hour or more has increased 1.96 times. The collapse and damage to soil structures caused by such heavy rain occur almost every year, and the risk of landslide disasters is increasing. In particular, embankment structures are earthen structures that are widely used in the construction of residential land, roads, railways, etc., and can be said to be social infrastructure structures that are indispensable to our lives. Therefore, it is necessary to suppress the damage caused by the collapse of the embankment because it causes a wide range of damage. Here, according to Road earthwork-embankment work guidelines [2], the safety of embankment structures against heavy rain strongly depends on four factors: Treatment of foundation ground, Quality of embankment material, Degree of compaction during construction, and Water drainage treatment. For this reason, countermeasures have been taken, as shown in Table 1. However, the current situation is that the factor analysis and the mechanism clarification of how the actual embankment structure collapses due to heavy rain are not sufficient, and this clarification is an urgent need. Therefore, in recent years, many model experiments have been conducted to reproduce embankment construction and rainfall, and factor analysis and mechanism clarification of embankment collapse are progressing [3][4]. However, it is difficult to grasp the stress state inside the embankment only by model experiments, and it is not possible to clarify the continuous stress state from construction to collapse, so it cannot be said to be a precise factor analysis.

Therefore, in this study, we conducted a model experiment to analyze the causes of embankment collapse and elucidate the mechanism. In addition to this, numerical analysis was carried out using the air-dissolved unsaturated soil/water/air-coupled finite analysis code [5] to reproduce the unsaturated ground, and an attempt was made to understand the continuous stress state from the time the embankment was constructed until it collapsed. Here, an analysis of embankment construction using this code has already been carried out [6][7][8]. However, at present, consistency between numerical analysis and actual phenomena has not been demonstrated, and it cannot be said that the results of numerical analysis are a fully reliable evaluation. Therefore, prior to understanding the stress state of the embankment due to heavy rain, we decided to perform a reproduction analysis of the model experiment in order to examine the usefulness of numerical analysis. Afterward, we investigated the stress state of the embankment due to heavy rain.

In this paper, we will explain the outline of the model experiment and numerical analysis and then report and discuss the results.

Table.1 Material parameters

Item	Treatment of foundation ground
Measure	Installation of Sand mats / Drainage trenches etc.
Item	Quality of embankment material
Measure	Understanding material properties Adjustment of water content ratio and particle size
Item	Degree of compaction during construction
Measure	Compaction management to improve deformation properties
Item	Water drainage treatment
Measure	Installation of drainage layer/drainage pipe

2. RESEARCH SIGNIFICANCE

Research has been conducted to clarify the causes of the collapse of embankment structures due to rainfall, but most of them focus on the collapse mode, and the stress state has not been fully understood. Under such circumstances, in this study, numerical analysis was adopted as a means of grasping the stress of the embankment due to rainfall, and an attempt was made to clarify this. Furthermore, the air-dissolved unsaturated soil/water/air-coupled finite analysis code [5] used in this study is one of the few analysis codes that can perform numerical analysis that reproduces unsaturated ground. From this point of view, this study is considered to be important for grasping the state of embankment structures due to rainfall.

3. MATERIALS AND METHODS

The model experiment was carried out using an acrylic soil tank with a length of 1,000 mm, a height of 700 mm, and a depth of 500 mm, as shown in Fig.1. The model embankment is a one-sided embankment with a height of 300mm and a top width of 210mm. The slope was set to 1:1.8 with reference to road earthwork-embankment work guideline [2]. The embankment material used in this test was a mixture of silica sand No. 3 and No. 8 for the foundation and silica sand No. 6, 7 and 8 for the embankment at a ratio of 5:2:5. In particular, the material for the embankment is classified as fine-grained sand (SF) according to triangular coordinate classification. From this, it can be said that this material has a poor composition and is prone to permeation and disintegration. Since the purpose of this experiment was to elucidate the causes of embankment collapse, this material was judged to be suitable for the test. In addition, the sample adjusted to 8.2% water content, which is the optimum water content obtained from the compaction test (JIS A 1210 A method) results, is used. The method of creating the model embankment is as follows (see Fig.2).

① After pouring out the material for the foundation ground, compaction is carried out until it reaches the specified thickness (Silica sand No. 3: 80 mm, Silica sand No. 8: 20 mm).

② Styrofoam is placed in a space other than the embankment.

③ A single layer of the sample with adjusted water content is laid out and compacted until it reaches the specified thickness.

④ ② and ③ are repeated for a total of 15 layers until the embankment height reaches 300 mm.

⑤ Incubate for one day.

⑥ Remove the styrofoam and shape the embankment slope using a straight knife.

After creating the model embankment, rainfall with the intensity of 80 mm/hour was applied until the embankment collapsed. In order to reproduce raindrops, rainfall was given using a device using hypodermic needle. In addition, as shown in Fig.1, the soil moisture meter and tensiometer installed inside the embankment were used to continuously measure the saturation and suction during the experiment. In addition, we tried to observe the collapse process and morphology of the embankment by constantly filming with a video camera.

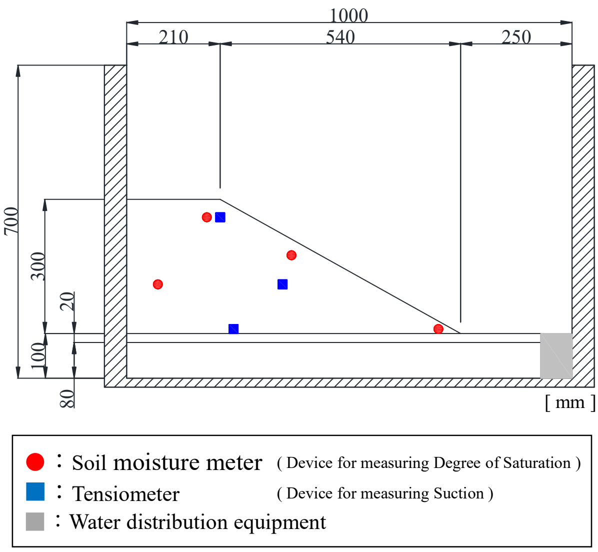

Fig.1 Standards for model experiments

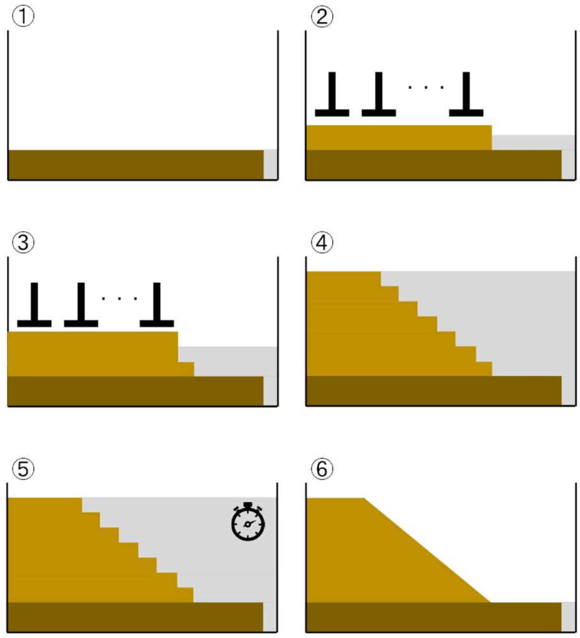

Fig.2 Model embankment creation flow

4. ANALYSIS METHODOLOGY

4.1. Air-Dissolved Unsaturated Soil / Water / Air Coupled Finite Analysis

4.1.1. About analysis code

Several unsaturated soil constitutive models have been proposed so far. In this study, we use the elasto-plastic constitutive model of unsaturated soil proposed by Ohno S., Kawai K., and Tachibana S. [9]. Ohno S., Kawai K. and Tachibana S. [9] proposed a model in which the effective saturation is the state quantity representing the stiffness, referring to the model in which the definition of the effective stress considering the water content of Karube D., Kato S. and Honda K. [10] is given.

In addition, it is widely known that the moisture characteristic curve (suction-saturation relationship), which determines the mechanical behavior of unsaturated soil, differs between dehydration and water absorption. In other words, there is not only one moisture characteristic curve that expresses the suction-saturation relationship, but there are countless scanning curves depending on the water retention state during dehydration or water absorption. Therefore, Kawai K., Wang W. and Iizuka A. [11] proposed a moisture characteristic curve model that can express hysteresis by using the fact that these scanning curves have similar shapes during dehydration and water absorption. In addition to the model capable of hysteresis expression, this analysis code uses the logistic curve equation as shown in the figure. Here, the Fig.3 is "(1) dehydration curve" and "(2) water absorption curve" drawn on the dehydration side and the water absorption side from an arbitrary suction-saturation state, which was proposed by Sugii T. and Uno T. [12].

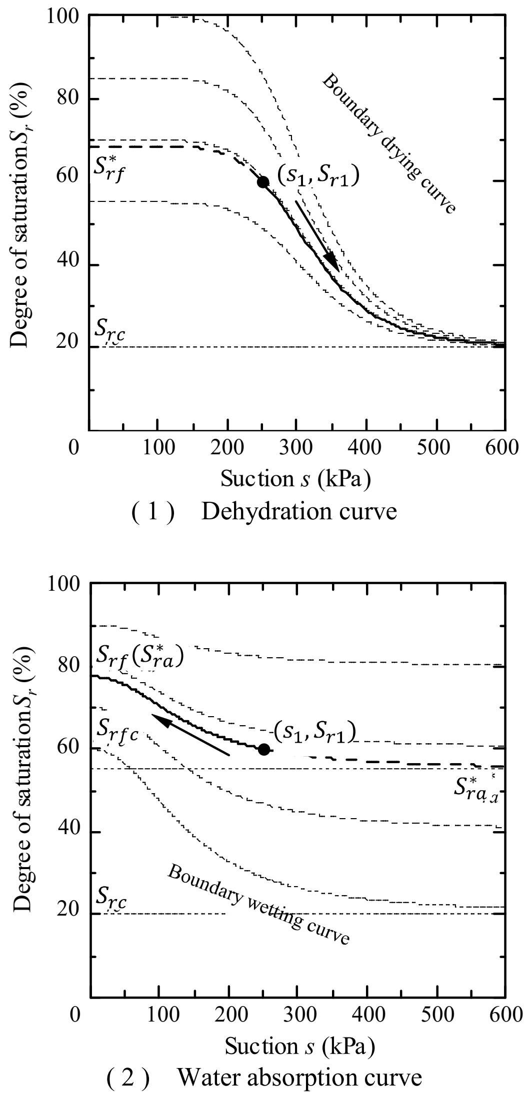

Fig.3 Moisture characteristic curve model

4.1.2. Finite element formulation

The governing equation in the unsaturated soil / water / air coupled problem consists of balanced ceremony, effective stress formula, unsaturated elasto-plastic constitutive equation, conformity expression, Darcy's rule, air Darcy's rule, continuous conditional expression, and continuous conditional expression considering gas phase, and is given by the following equations.

<u>Balanced ceremony</u>

$$\mathrm{div}\boldsymbol{\sigma}^T + \rho\mathbf{g} = 0, \quad \boldsymbol{\sigma} = \boldsymbol{\sigma}^T \tag{1}$$

<u>Effective stress formula</u>

$$\boldsymbol{\sigma}' = \boldsymbol{\sigma}^N + p_s\mathbf{1}, \quad \boldsymbol{\sigma}^N = \boldsymbol{\sigma} - p_a\mathbf{1} \tag{2}$$

Unsaturated elasto-plastic constitutive equation

$$\dot{\boldsymbol{\sigma}}' = \mathbf{D} : \dot{\boldsymbol{\varepsilon}} - \mathbf{C}^S \dot{S}_e \tag{3}$$

Conformity expression

$$\boldsymbol{\varepsilon} = -\frac{1}{2}\left(\nabla \mathbf{u}\right)^S \tag{4}$$

Darcy's rule

$$\tilde{\boldsymbol{v}} = -\mathbf{k} \cdot \mathrm{grad}h \tag{5}$$

Air Darcy's rule

$$\tilde{\boldsymbol{v}}_a = -\mathbf{k}_a \cdot \mathrm{grad}p_a \tag{6}$$

Continuous conditional expression

$$n\dot{S}_\mathrm{r} - S_\mathrm{r}\dot{\varepsilon}_v + \mathrm{div}\tilde{\boldsymbol{v}} = 0 \tag{7}$$

Continuous conditional expression considering gas phase

$$(1-S_\mathrm{r})\dot{\varepsilon}_v + n\dot{S}_\mathrm{r} - n(1-S_\mathrm{r})\frac{\dot{p}_a}{K_a} - \mathrm{div}\tilde{\boldsymbol{v}}_a = 0 \tag{8}$$

Here, assuming that the saturation is a function that can be expressed only by suction, the following equation is obtained.

$$\dot{S}_\mathrm{r} = \frac{dS_\mathrm{r}}{ds}\dot{s} = -\frac{dS_\mathrm{r}}{ds}\dot{p}_w \tag{9}$$

In addition, the increment of suction stress in Equation (2) is calculated by the following equation.

$$\begin{aligned} \dot{p}_s &= \frac{\dot{S}_\mathrm{r}}{1-S_{\mathrm{r}c}}s + \frac{S_\mathrm{r} - S_{\mathrm{r}c}}{1-S_{\mathrm{r}c}}\dot{s} \\ &= \frac{1}{1-S_{\mathrm{r}c}}\left(\frac{dS_\mathrm{r}}{ds}s + S_\mathrm{r} - S_{\mathrm{r}c}\right)\dot{s} \end{aligned} \tag{10}$$

However, S_{rc} is considered to be the saturation degree indicated by the adsorbed aqueous phase, and is a material constant.

Here, $\boldsymbol{\sigma}'$ is the effective stress tensor; $\boldsymbol{\sigma}^N$ is the base stress tensor; $\boldsymbol{\sigma}$ is the total stress tensor; p_s is the suction stress; p_a is the pore air pressure; $\mathbf{D}$ is the elastic stiffness tensor; $\boldsymbol{\varepsilon}$ is the strain tensor; $\mathbf{C}^S$ is the coefficient tensor; S_e is the effective degree of saturation; $\mathbf{u}$ is the displacement vector; $\tilde{\boldsymbol{v}}$ is the flow velocity vector of interstitial water; $\mathbf{k}$ is the permeability coefficient tensor; h is the all head; S_r is the degree of saturation; ε_v is the volumetric strain; n is the porosity; K_a is the air pressure; $\tilde{\boldsymbol{v}}_a$ is the flow velocity vector of interstitial air; and the superscript s indicates the symmetric part of the tensor in ( ).

By weakly formalizing the above governing equation, discretizing it spatially and temporally, and solving it under the conditions of initial value and boundary value, the solutions of unknowns $\left\{\Delta\mathbf{u}^N\right\}$, $\left\{\Delta\mathbf{h}^N\big|_{t=t+\Delta t}\right\}$, and $\left\{\Delta\mathbf{p}_\mathbf{a}^N\big|_{t=t+\Delta t}\right\}$ can be obtained.

Here, $\Delta\mathbf{u}^N$ is the amount of change in node displacement; $\Delta\mathbf{h}^N$ is the amount of change in total head in minute time Δt ; $\Delta\mathbf{p}_\mathbf{a}^N$ is the amount of change in air pressure in a minute time Δt.

4.2. Analysis Conditions

Numerical analysis was carried out for the purpose of understanding the stress behavior of the embankment due to rainfall infiltration. However, unless the consistency between actual phenomena and numerical analysis is shown, it is difficult to say that the results of numerical analysis are sufficiently reliable. Therefore, in this study, first, we performed a reproduction analysis of the model experiment mentioned earlier and examined the usefulness of the numerical analysis. After that, we grasped the stress behavior of the embankment.

Fig.4 shows the reproduction analysis model. This reproduction analysis model was set according to the size of the model in the model experiment (see Fig. 1). The materials used were the same for the embankment and foundation, and each parameter was set according to the material of the embankment in the model experiment. Table.2 shows the material parameters, and Fig.5 shows the moisture characteristic curve. Regarding the material parameters, λ is the expansion index; κ is the compression index; M is the limit state parameter; m is the unsaturated permeability coefficient of Mualem [13]; n is the E_c model parameter; n_E is the enlargement ratio of yield surface; ν is the Poisson's ratio; S_{rc} is the critical degree of saturation; S_{r0} is the initial degree of saturation; e_0 is the initial void ratio; $k_{x,y}$ is the hydraulic conductivity [m/sec]; $k_{ax,ay}$ is the coefficient of air permeability [m/sec]; ρ_s is the soil particle density [t/m^3]; ρ_t is the wet density[t/m^3] and ρ_a is the air density [t/m^3].

In the reproduction analysis, we performed a construction analysis that reproduced compaction in accordance with the model experiment, and then performed a rainfall analysis. The analysis flow is as follows (see Fig.6).

① Generate foundation ground.

② Generate elements for one layer of embankment. (Spreading part)

③ After applying a load equivalent to 10kPa to the upper side of the generated element, remove the load equivalent to 10kPa from the same element and at the same location. (Compaction part)

※ Regarding the loading and unloading loads, the values obtained by converting the dynamic compaction energy during the model experiment into static energy were used.

④ Repeat step ③ a total of 5 times.

※ The number of compactions was set according to the number of compactions in the model experiment.

⑤ Repeat steps ② to ⑤ until the embankment height is 300mm.

⑥ Apply rain with a rainfall intensity of 80mm/hour to the top of the embankment and the top of the slope foundation ground.

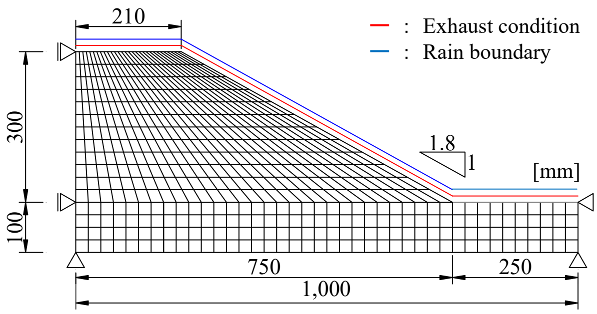

Fig.4 Finite element analysis model

Table.2 Material parameters

λ	κ	M
0.025	0.0025	1.33
m	n	n_E
0.80	1.0	1.3
ν	S_{rc}	S_{r0}
0.33	0.15	0.30
e_0	$k_{x,y}$ [m/sec]	$k_{ax,ay}$ [m/sec]
0.70	1.0×10^{-4}	1.0×10^{-2}
ρ_s [t/m³]	ρ_t [t/m³]	ρ_a [t/m³]
2.610	1.605	0.0012

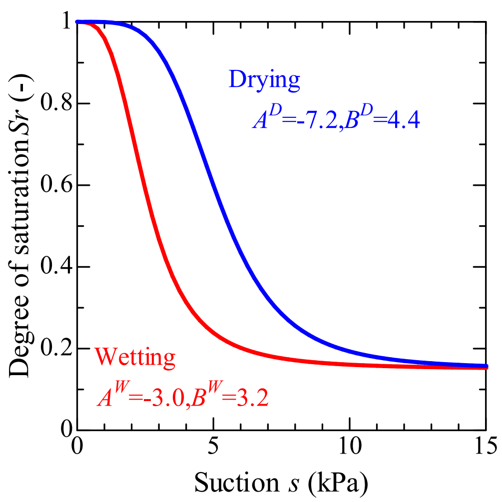

Fig.5 Moisture characteristic curve

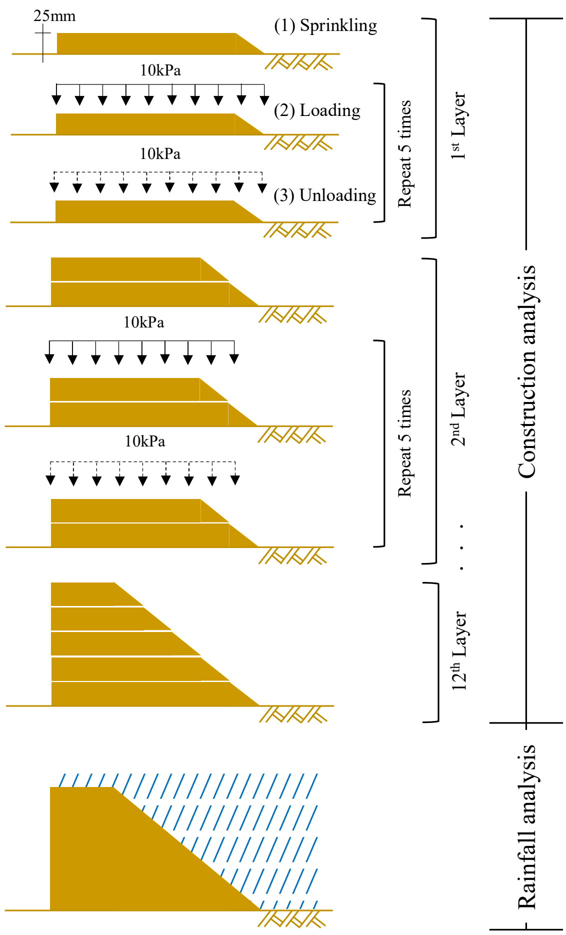

Fig.6 Reproduction analysis flow

5. RESULT AND DISCUSSION

5.1 Collapse Process of Embankment due to Rainfall

In this section, we examine the collapse process and collapse mode of the embankment due to rainfall through the results of model experiments.

Fig.7 (i) shows the time course of suction and saturation in the model experiment. First, looking at the change in the suction over time, it was confirmed that the suction decreased significantly near the top of slope (●) immediately after rain infiltration, and then decreased in the order of the inside of the embankment (▽) and the deep part of the embankment (×). Looking at the change in the degree of saturation over time, it was confirmed that the saturation progressed near the toe of the slope (▲) immediately after rainfall, followed by saturation on the slope (●, ■) and the deep part of the embankment (◇), and that the wide area of the embankment was saturated in approximately 40 minutes. In addition, when comparing the two, it was confirmed that the timing of the suction decrease and the timing of the saturation increase were almost the same, for example, near the top of the slope (●) and in the deep part of the embankment (◇,×). From this result, it was suggested that the embankment becomes a weak part due to the decrease in suction caused by the increase in saturation.

Fig.8 shows how the model embankment collapsed. Looking at this, erosion due to rainfall was confirmed at the toe and base of the slope about 15 minutes after the start of rainfall. Furthermore, after about 50 minutes, the foundation became completely saturated and the model embankment began to collapse from the toe of the slope, and it was confirmed that the collapse progressed in the direction of the shoulder of the slope.

As described above, rainfall experiments using a model embankment confirmed that the decrease in suction and the increase in saturation due to rainwater infiltration progressed from the vicinity of the slope, leading to collapse from the vicinity of the toe of the slope.

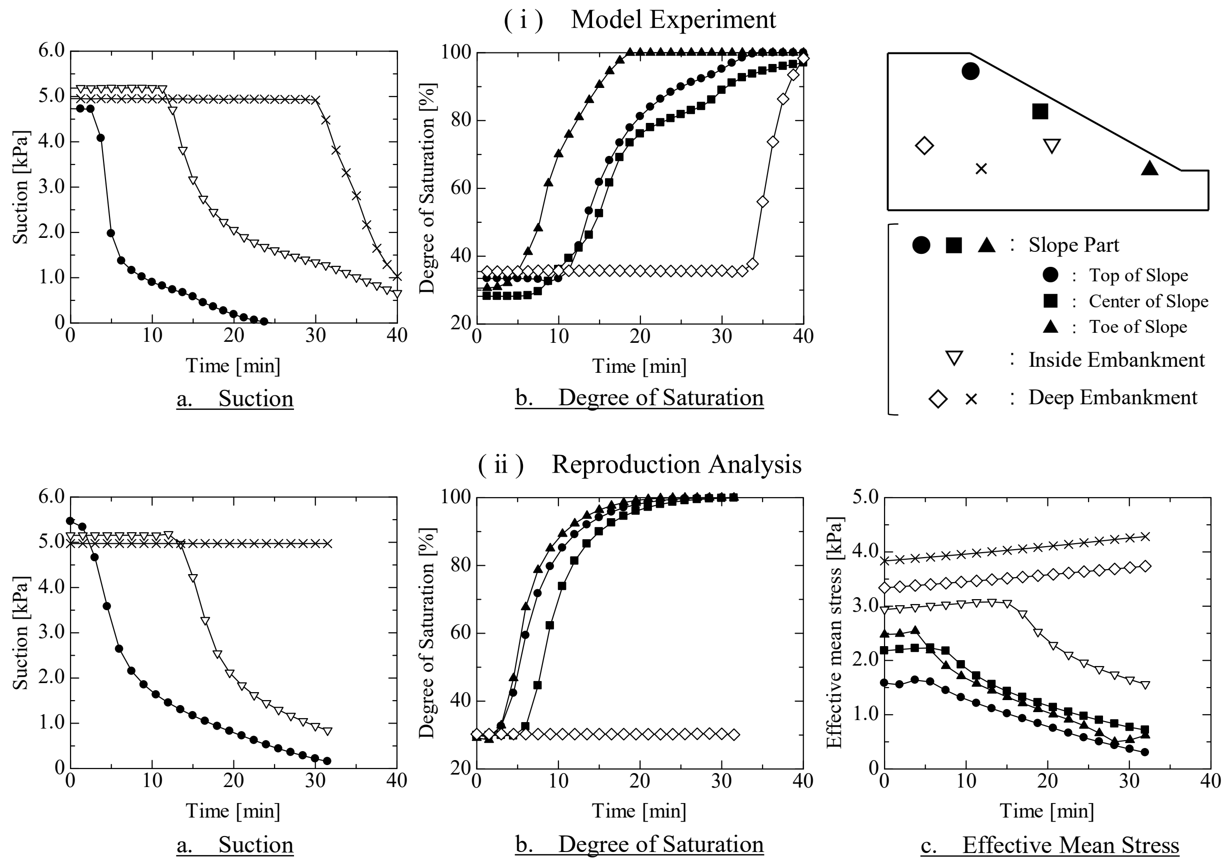

Fig.7 Model experiment and reproduction analysis results

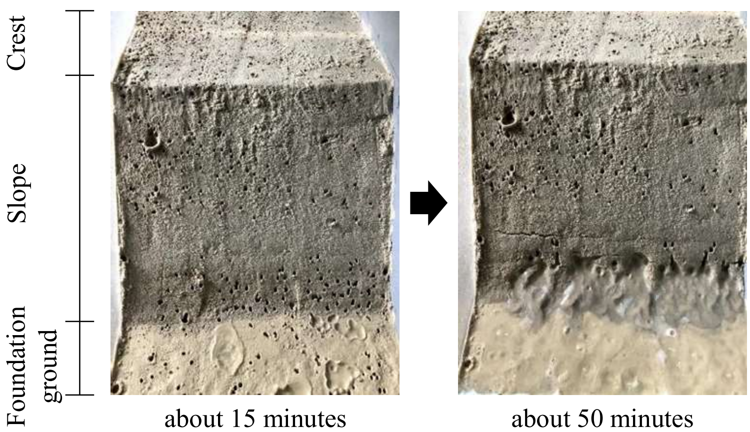

Fig.8 Destruction mode of model embankment

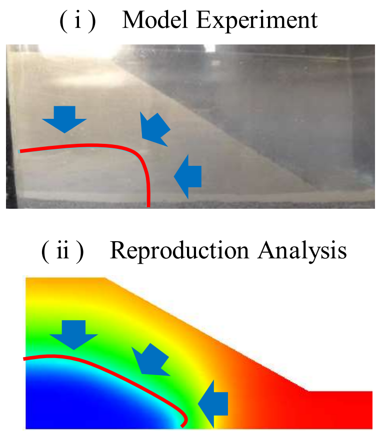

Fig.9 Appearance of infiltrated surface

5.2 Examination of Usefulness of Numerical Analysis

In this section, we examine the usefulness of numerical analysis based on the model test results and reproduction analysis results in the previous section.

Fig.7 (ii-a,b) shows the temporal changes in suction and saturation in the model experiment reproduction analysis. First, looking at the change in suction over time, it was confirmed that the suction decreased significantly near the top of the slope (●) immediately after rain infiltration, followed by a decrease in the inside of the embankment (▽) and then in the deeper part of the embankment (×). This is the same behavior as the model experiment. In addition, the timing at which the suction decreased in each element was almost the same between the model test and the simulation analysis, confirming qualitative agreement between the two.

Looking at the change in the degree of saturation over time, it was confirmed that the saturation increased near the slope immediately after rain infiltration, and it was confirmed that the same behavior as the model experiment results was shown. This analysis is designed to end when the suction at a certain element becomes 0. Therefore, the increase in the degree of saturation cannot be confirmed in the deep part of the embankment (◇). However, since the saturation degree is constant for about 30 minutes from rainfall infiltration, both of them agree, so it is considered that the saturation degree is also qualitatively consistent as with suction.

Fig.9 shows the appearance of formation on the infiltration surface in model experiments and reproduction analysis. It can be seen that the formation of the infiltration surface progressed from the embankment crest/slope to the inside of the embankment in both cases, and good agreement was confirmed between the two.

As described above, we were able to confirm qualitative agreement between the model experiment and the reproduction analysis in terms of three points, namely, changes in suction and degree of saturation over time, and the appearance of infiltration surface formation. Therefore, we were able to obtain consistency between actual phenomena and numerical analysis. From this, it can be said that the usefulness of the numerical analysis was demonstrated.

5.3 Stress Behavior of Embankment under Rainfall

In the previous section, we showed the usefulness of numerical analysis through reproduction analysis of model experiments. In this section, we grasp the stress state of the embankment due to rainfall.

Fig.7 (ii-c) shows the temporal change of the effective stress in the model test reproduction analysis. Looking at this, it can be confirmed that the stress decreases on the slope (●, ■, ▲) and inside the embankment (▽). The timing at which the stress decreases roughly coincides with the timing at which the suction decreases or the degree of saturation increases in Fig.7. From this, it became clear that stress decreased due to a decrease in suction and an increase in saturation due to rainfall infiltration, and the embankment weakened and collapsed. In addition, the toe of the slope and its vicinity (▲, ▽) show a greater decrease in stress than the center of the slope and the shoulder of the slope, indicating that the toe of the slope is particularly vulnerable. This is consistent with the collapse near the bottom of the slope in the model experiment.

From this, we believe that understanding the stress state using numerical analysis will help clarify the weakening process and collapse mechanism of the embankment.

6. CONCLUSIONS

In this study, ① Factor analysis and clarification of the mechanism of embankment failure by model experiments, ② Examination of the usefulness of numerical analysis by reproduction analysis of model experiments, and ③ Examination of the stress state of the embankment due to rainfall through numerical analysis, were performed. As a result, knowledge was obtained.

(1) According to the model embankment and the measurement method adopted in this experiment, it was confirmed that the suction of the embankment structure decreased and the degree of saturation increased from the slope to the inside due to rainfall. As a result, it became clear that the collapse progresses from the bottom of the slope.

(2) In the reproduction analysis of the model experiment, we were able to confirm good agreement between the three points of suction, saturation, and infiltration surface. As a result, the air-dissolved unsaturated soil/water/air coupled finite analysis code [5] used in this analysis was able to reproduce actual phenomena at a high level, demonstrating the usefulness of numerical analysis.

(3) Numerical analysis of the stress behavior confirmed a large stress drop, especially near the toe of the slope, and obtained results consistent with the collapse morphology in model experiments. From this, it was shown that understanding the stress state by numerical analysis would help clarify the weakening process and collapse mechanism of the embankment.

In the future, we plan to expand the analysis model to a full-scale model and try to understand the stress state under various conditions.

7. REFERENCES

[1] Japan Meteorological Agency, http://www.jma.go.jp/jma/index.html.

[2] Japan road association, Road earthwork-embankment work guidelines, MARUZEN publishing, 2010, pp.1-310.

[3] Kawajiri S., Nunokawa O., Itoh Y., Nishida M., Matsumaru T., Kawaguchi T., Ota N. and Sugiyama T., Experimental study of embankment collapse mechanism due to rainfall after earthquake, Geotechnical Engineering Journal, Vol.9, No.2, 2013, pp.153-168.

[4] Ichii K., Experiment study on seismic resistance reduction of embankment due to rainfall, JSCE journal of Earthquake Engineering, Vol.28, 2005, pp.188-195.

[5] Kanazawa S., Toyoshima K., Kawai K., Tachibana S. and Iizuka A., Analysis of mechanical behavior of compacted soil with F.E. method, journal of JSCE, No.68 (2), 2012, pp.291-298.

[6] Kanazawa S. and Suzuki S., Stress analysis of embankment due to different in construction condition, International Journal of GEOMATE, Vol.18, Issue 65, 2020, pp. 1 – 8.

[7] Nakamura E. and Kanazawa S., Analytical study on quality evaluation of embankment structure with a view to longer life, International Journal of GEOMATE, Vol.20, Issue 78, 2021, pp.177-182.

[8] Kanazawa S. and Igarashi H., Analysis of embankment stress produced during construction and in-service phases considering embankment geometries, International Journal of GEOMATE, Vol.20, Issue 79, 2021, pp.68-73.

[9] Ohno S., Kawai K. and Tachibana S., Elasto-plastic constitutive model for unsaturated soil applied effective degree of saturation as a parameter expressing stiffness, journal of JSCE, Vol.63/No.4, 2007, pp.1132-1141.

[10] Karube D., Kato S., Hamada K. and Honda M., The relationship between the mechanical behavior and the state of porewater in unsaturated soil, journal of JSCE, No.535/III-34, 1996, pp.83-92.

[11] Kawai K., Wang W. and Iizuka A., The expression of hysteresis appearing on water characteristic curves and the change of stresses in unsaturated soils, Journal of applied mechanics, Vol.5, 2002, pp.777-784.

[12] Sugii T. and Uno T., Modeling the New Moisture Characteristic Curve, Journal of JSCE, 1995, pp.130-131.

[13] Mualem Y., A new model for predicting the hydraulic conductivity of unsaturated porous media, Water Resources Research, Vol.12, No.3, 1976, pp.514-522.